

1 **Expanding the repertoire of GalNAc analogues for cell-specific bioorthogonal**
2 **tagging of glycoproteins**

3

4 Abdul Zafar^{1,2}, Sandhya Sridhar^{1,2,3}, Ganka Bineva-Todd², Anna Cioce^{1,2}, Nadia
5 Abdulla^{1,2}, Vincent Chang⁴, Stacy A. Malaker⁴, David S. Hewings⁵, Benjamin
6 Schumann^{1,2*}

7

8 ¹ Department of Chemistry, Imperial College London, W12 0BZ London, United
9 Kingdom.

10 ² Chemical Glycobiology Laboratory, The Francis Crick Institute, NW1 1AT London,
11 United Kingdom.

12 ³ Tumour-Host Interaction Laboratory, The Francis Crick Institute, NW1 1AT London,
13 United Kingdom.

14 ⁴ Department of Chemistry, Yale University, CT 06511 New Haven, United States.

15 ⁵ Vertex Pharmaceuticals (Europe) Ltd., 86-88 Jubilee Avenue, Milton Park,
16 Abingdon, Oxfordshire OX14 4RW, United Kingdom.

17 *Correspondence: b.schumann@imperial.ac.uk

18

19

20 **Abstract**

21 Glycosylation is a ubiquitous modification of proteins, necessitating approaches for
22 visualization and characterization. Bioorthogonally tagged monosaccharides have
23 been instrumental to this end, offering a chemical view into the cell biology of
24 glycans. Understanding the use of such monosaccharides by cellular biosynthetic
25 pathways has expanded their applicability in cell biology, for instance through the
26 strategy Bioorthogonal Cell-specific Tagging of Glycoproteins (BOCTAG). Here, we
27 show that the cellular use of two azide-tagged analogues of the monosaccharide *N*-
28 acetylgalactosamine can be promoted through expression of two biosynthetic
29 enzymes. Cellular expression of the kinase NahK and the engineered
30 pyrophosphorylase AGX1^{F383A} led to biosynthesis of the corresponding activated
31 nucleotide-sugars and subsequent bioorthogonal tagging of the cellular
32 glycoproteome. We explore the use of both sugars for BOCTAG, demonstrating the
33 visualization of cell surface glycosylation in a specific cell line in a co-culture system.
34 Our work adds to the toolbox of glycoprotein analysis in biomedicine.

35 Introduction

36 The proteome is substantially expanded through posttranslational modifications
37 (PTMs). Glycosylation is the most abundant and complex PTM, and tools to
38 understand the glycoproteome are thus essential to contribute to understanding in
39 biology. Bioorthogonal chemistry was first developed to study glycosylation due to
40 the lack of genetic methods to directly manipulate glycans. Glycobiology has since
41 played a key role in enhancing bioorthogonal chemistry.

42 A number of monosaccharides have been furnished with chemical tags to allow for
43 bioorthogonal incorporation of reporter compounds such as fluorophores or
44 enrichment reagents. Azide groups were among the first such tags, as they are inert
45 to cellular metabolic processes and are amenable to copper-catalysed (CuAAC) or
46 strain-promoted azide-alkyne (SPAAC) cycloaddition reactions to append reporter
47 groups such as fluorophores.¹⁻⁴ Other tags have included alkynes, alkenes, and
48 many others that are suitable for distinct bioorthogonal reactions.⁴⁻¹³ The successful
49 use of tagged monosaccharides relies on their acceptance by biosynthetic enzymes
50 to generate UDP-sugars, and on glycosyltransferases using these UDP-sugars as
51 substrates. Appending an azido group to the side chain of *N*-acetylgalactosamine
52 (GalNAc) or *N*-acetylglucosamine (GlcNAc) to render GalNAz or GlcNAz,
53 respectively, allows acceptance by both types of enzymes and incorporation into the
54 glycoproteome.¹⁴⁻¹⁶ However, even slightly bigger modifications can render
55 monosaccharides refractory to incorporation (Fig. 1A).^{2,17-20}

56 We and others have found that acylamide moieties in GalNAc and GlcNAc with
57 sterically more demanding modifications are often not converted to the
58 corresponding UDP-sugar analogues. In parallel with Chen and colleagues, we have
59 shown that UDP-sugar biosynthesis can be engineered into a cell line for cell-
60 selective incorporation in co-culture systems alongside more advanced *in vivo*
61 systems.^{17,20,21} This strategy, termed Bio-Orthogonal Cell-specific TAGging of
62 Glycoproteins (BOCTAG), employs the bacterial sugar-1-kinase NahK that is more
63 promiscuous towards chemical modifications than the human kinases GALK1 and
64 GALK2.^{17,22} An engineered human pyrophosphorylase AGX1^{F383A} then converts
65 GalNAc-1-phosphates to UDP-GalNAc analogues.^{2,18,21,23,24} Chen and colleagues
66 used the similarly engineered (F383G) pyrophosphorylase AGX2, an isoenzyme to
67 AGX1, along with a bioorthogonal GlcNAc analogue to mediate UDP-sugar
68 biosynthesis.²⁰ Both studies employed linear alkynoate side chains as bioorthogonal

69 tags, either a pentynoate side chain e.g. in the sugar GalNAk, or a hexynoate side
70 chain in the sugar GalN6yne. The corresponding UDP-GalNAc analogues are
71 interconverted into the corresponding UDP-GlcNAc analogues and vice versa by the
72 activity of the epimerase GALE, leading to labelling of various sub-types of the
73 glycome. However, only a limited set of sugars have been used to this end. A set of
74 bioorthogonal sugars with alternative chemical tags and potential incorporation into
75 different sub-sections of the glycome would be useful to expand our repertoire of
76 tools to study the glycoproteome.

77 We have previously identified the bioorthogonal azide-containing GalNAc analogue
78 GalNAzMe to be selectively incorporated into O-GalNAc glycans (Fig. 1A).²
79 Selectivity was conferred by the branched nature of the acylamide modification,
80 rendering the corresponding nucleotide-sugar UDP-GalNAzMe resistant to cellular
81 epimerisation by GALE to the respective analogue termed UDP-GlcNAzMe.² In
82 contrast, the nucleotide-sugar UDP-GalNPrAz, an isomer of UDP-GalNAzMe with a
83 linear acylamide, was epimerised to UDP-GlcNPrAz *in vitro*. While no cellular
84 labelling studies with GalNPrAz were attempted at the time, we reasoned that
85 GalNPrAz may be a more promiscuous metabolic chemical reporter of glycosylation.
86 Testing these hypotheses was challenging at the time since biosynthesis of UDP-
87 GalNAzMe in cells was only possible from a synthetically complex caged sugar-1-
88 phosphate in cells expressing AGX1^{F383A}.^{2,21} Our later findings suggesting that the
89 kinase NahK can prime the biosynthesis of chemically tagged UDP-sugars led us to
90 evaluate the metabolic fate of GalNAzMe and GalNPrAz (Fig. 1A). Here, we
91 demonstrate that the BOCTAG principle can be expanded to allow biosynthesis and
92 use of UDP-GalNAzMe and UDP-GalNPrAz from synthetically accessible precursors
93 to increase the variability of metabolic reporters for cell-selective glycoproteome
94 evaluation.

95

96 **Results and Discussion**

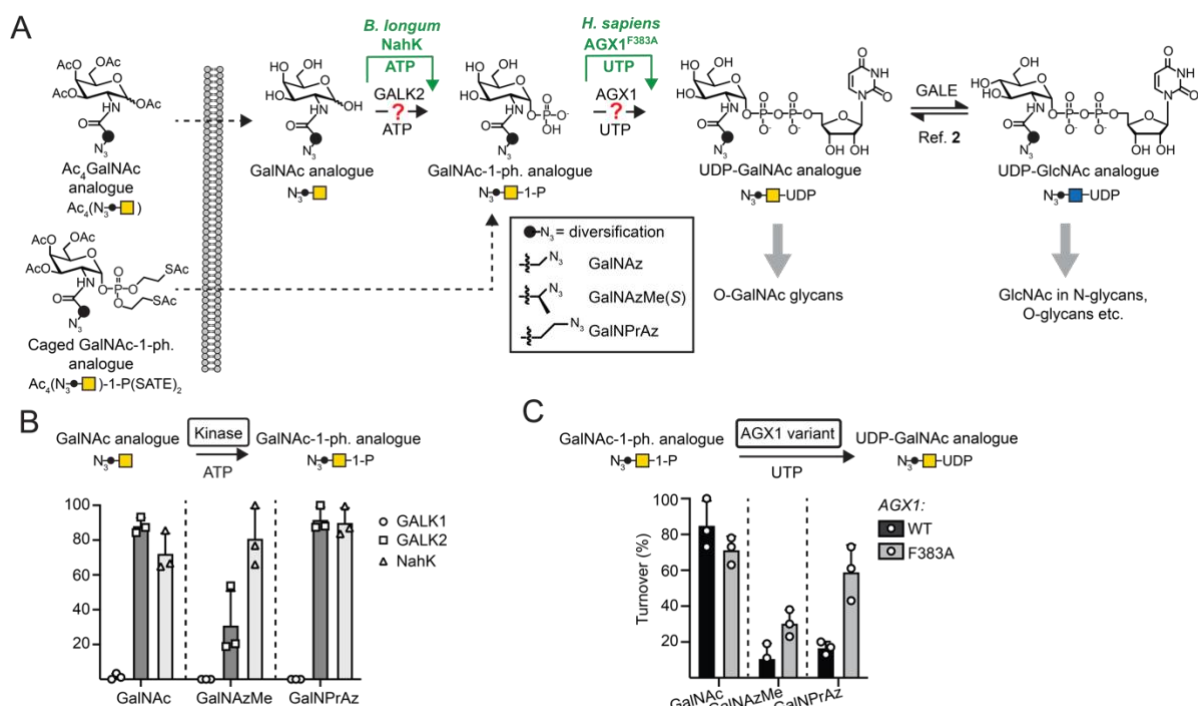
97

98 ***In vitro* enzymatic synthesis of chemically modified UDP-GalNAc analogues**

99

100 To anticipate cellular biosynthesis, we investigated how GalNPrAz and GalNAzMe
101 can be enzymatically converted to their respective UDP-GalNAc analogues. We first

102 subjected each monosaccharide alongside GalNAc to recombinant human kinases
103 GALK1, GALK2 or the bacterial kinase NahK and measured turnover to sugar-1-
104 phosphates by ultra-performance liquid chromatography with mass spectrometry
105 detection (UPLC-MS) after either 3 h or 16 h reactions (Fig. 1B, Supporting Fig. 1).
106 GALK2 accepted both GalNAc and GalNPrAz as substrates to afford > 60% and
107 near-complete turnover in 3 h and 16 h reactions, respectively. In contrast,
108 conversion of GalNAzMe by GALK2 proceeded slowly and with approximately 3-
109 times lower turnover after a 16 h reaction. The more promiscuous kinase NahK
110 accepted all three substrates, with > 80% conversion of the synthetic compounds
111 GalNAzMe and GalNPrAz after 16 h (Fig. 1B). The galactose-specific kinase GALK1
112 did not accept any of the three monosaccharides, in line with our previous findings
113 on GalNAc analogues.¹⁷ We next assessed conversion of sugar-1-phosphates to
114 UDP-sugars by AGX1^{F383A} (Fig. 1C, Supporting Fig. 2). Monosaccharides were
115 converted to sugar-1-phosphates by NahK *in situ* and treated in a one-pot
116 multienzyme (OPME) reaction with 125 nM WT-AGX1 or AGX1^{F383A}. Measuring
117 UDP-sugar biosynthesis by UPLC with UV detection, we found that WT-AGX1 used
118 chemically modified GalNAc analogues with lower turnover (< 20%) compared to
119 GalNAc (91%). In contrast, AGX1^{F383A} yielded a 67% turnover for UDP-GalNPrAz
120 and 27% turnover for UDP-GalNAzMe in a 16h reaction (Fig. 1C). The *in vitro*
121 turnover reactions by AGX1 variants matched our previous cellular biosynthesis
122 data.² Reactions stopped after 3 h showed generally low turnover, with the same
123 trends as observed for 16 h reactions (Supporting Fig. 2A). We tested a higher
124 concentration of 500 nM recombinant AGX1 to corroborate these results (Supporting
125 Fig. 2B). Including alkyne-tagged GalNAc analogues GalNAIk and GalN6yne in
126 OPME reactions (Supporting Fig. 2C), we similarly found that NahK together with
127 AGX1^{F383A} produced the corresponding UDP-sugars in near-quantitative turnover in
128 3 h and 16 h reactions.^{17,21,24} Taken together, the combination of the enzymes
129 NahK/AGX1^{F383A} that featured in our BOCTAG approach successfully synthesised a
130 range of chemically modified UDP-GalNAc analogues from free monosaccharides.
131



132

133 **Fig. 1:** Engineered biosynthesis for UDP-GalNAc analogues. **A**, biosynthetic pathways. UDP-GalNAc
 134 is biosynthesized by GALK2 and AGX1 activities, while modifications often require the enzymes NahK
 135 and AGX1^{F383A}. **B**, acceptance of GalNAc as well as azide-tagged analogues by sugar-1-kinases as
 136 measured by UPLC-MS in 16 h reactions. Data are means + SD from three independent replicates. **C**,
 137 acceptance of GalNAc-1-phosphate as well as azide-tagged analogues by AGX1 constructs as
 138 assessed by UPLC. GalNAc-1-phosphate analogues were generated *in situ* by reaction of the
 139 corresponding monosaccharides with NahK as shown in **B**. Data are means + SD from three
 140 independent replicates.

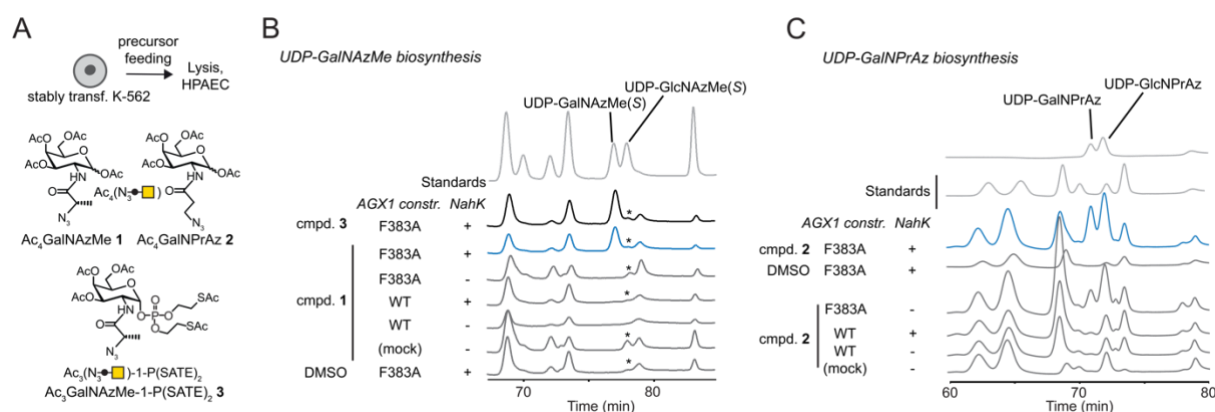
141

142 Cellular biosynthesis of UDP-GalNAzMe and UDP-GalNPrAz

143

144 We assessed biosynthesis in K-562 cells expressing combinations of NahK and
 145 AGX1 constructs. Per-acetylated sugars Ac₄GalNAzMe **1** and Ac₄GalNPrAz **2** were
 146 used as synthetically convenient monosaccharide precursors (Fig. 2A). A caged
 147 GalNAzMe-1-phosphate **3** previously used by us was employed as a control for
 148 biosynthesis.² Mindful that high concentrations of per-acetylated compounds can
 149 lead to non-enzymatic background labelling even without UDP-sugar
 150 biosynthesis,^{25,26} we included a control cell line transfected with an empty plasmid
 151 not encoding either of the biosynthetic enzymes. Cells were fed with sugar
 152 precursors, and UDP-sugar biosynthesis was assessed by high performance anion
 153 exchange chromatography (HPAEC) (Fig. 2A, B).^{2,18} Comparison with synthetic
 154 standards indicated that cells expressing both NahK and AGX1^{F383A} biosynthesized

155 UDP-GalNAzMe from Ac₄GalNAzMe **1** alongside GalNAzMe-1-phosphate **3** (Fig.
 156 2B). Both NahK and AGX1^{F383A} were needed for UDP-GalNAzMe biosynthesis from
 157 Ac₄GalNAzMe, as cell lines expressing only one of the components or
 158 overexpressing WT-AGX1 did not yield a peak at the corresponding retention time
 159 (Fig. 2B). Our previous work on the biosynthetic fate of tagged monosaccharides
 160 indicated that branched acylamide side chains such as in UDP-GalNAzMe suppress
 161 epimerization between UDP-GalNAc analogues and UDP-GlcNAc analogues.² We
 162 therefore included the synthetic compound UDP-GlcNAzMe as a standard in our
 163 HPAEC experiments.² We could not conclusively rule out epimerisation of UDP-
 164 GalNAzMe in these experiments since a peak with variable intensity from cell lysates
 165 eluted at the retention time of UDP-GlcNAzMe (Fig. 2B, asterisk). Feeding cells with
 166 increasing concentrations of Ac₄GalNAzMe **1** did not correlate with increasing
 167 intensity of this peak (Supporting Fig. 3A). We therefore concluded that
 168 epimerization of UDP-GalNAzMe was not detectable in our assay.² UDP-GalNPrAz
 169 was successfully biosynthesized in cells expressing NahK and AGX1^{F383A}, although
 170 small amounts were produced in the absence of NahK (Fig. 2C, Supporting Fig. 3B).
 171 Including the corresponding UDP-GlcNAc analogue which we termed UDP-
 172 GlcNPrAz as a standard, we observed clear epimerization of UDP-GlcNPrAz in cells,
 173 although the corresponding peak likewise overlapped with a background peak (Fig.
 174 2C, Supporting Fig. 3B). Taken together, these data suggested that the presence of
 175 the BOCTAG enzymes is an efficient way to biosynthesize both UDP-GalNAzMe and
 176 UDP-GalNPrAz.



177
 178 **Fig. 2:** Engineered cellular biosynthesis of UDP-GalNAzMe and UDP-GalNPrAz. **A**, experimental
 179 layout and synthetic compounds used. **B**, biosynthesis of UDP-GalNAzMe in stably transfected cells
 180 as measured by HPAEC. Cells were fed with 50 μ M synthetic compounds or DMSO. Data are from
 181 one representative out of at least two replicates. Asterisk denotes a peak likely due to an artifact of

182 chromatography conditions. C, biosynthesis of UDP-GalNPrAz in stably transfected cells as
183 measured by HPAEC. Cells were fed with 50 μ M compound **2** or DMSO. Data are from one
184 representative out of at least two replicates.

185

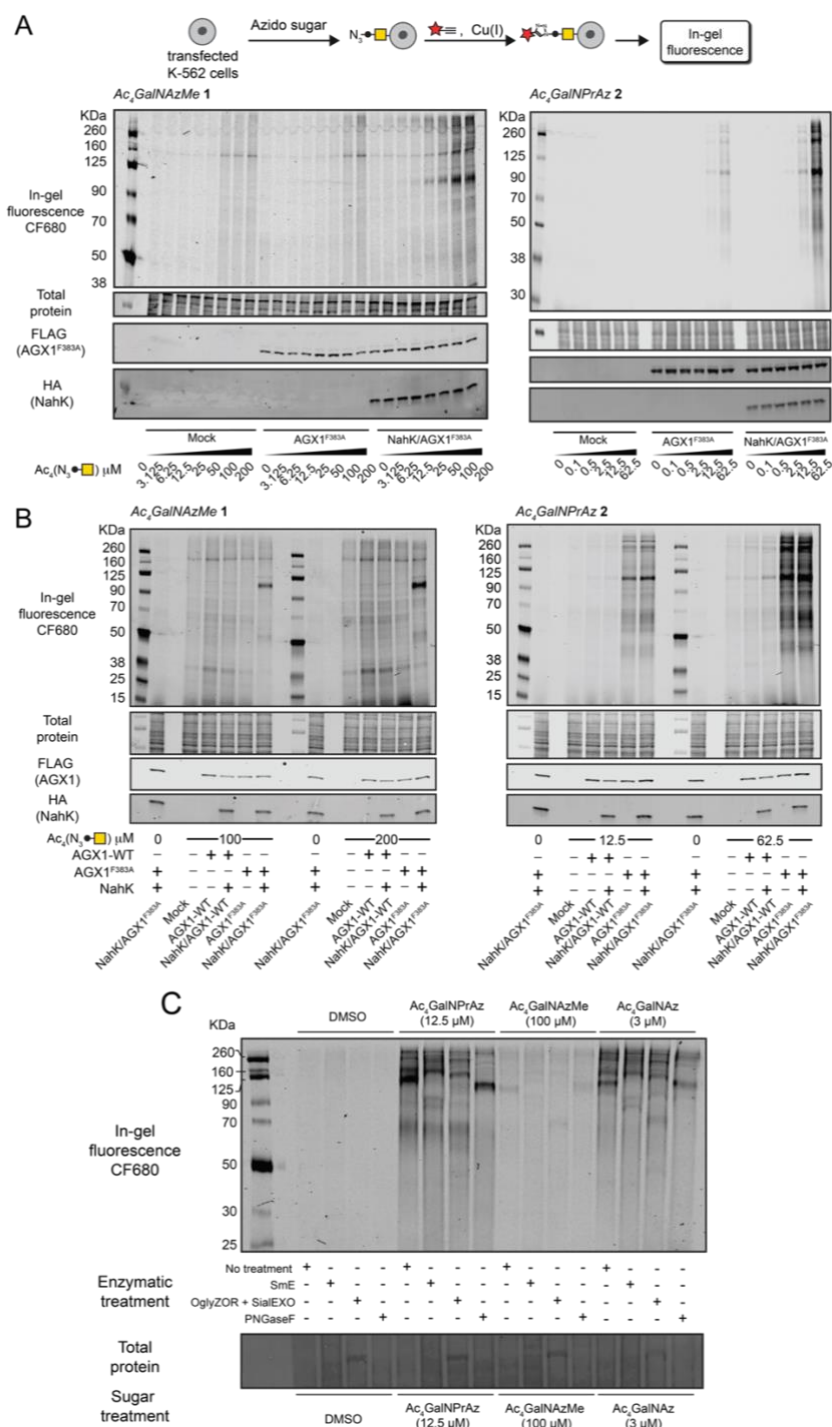
186 **Incorporation of GalNAzMe and GalNPrAz into cell-surface glycoproteins**

187

188 We assessed incorporation of GalNAc analogues into cellular glycans by on-cell
189 CuAAC with a near-infrared fluorophore. This experimental setup ensured that only
190 cell surface glycosylation was detected by ensuing in-gel fluorescence of
191 lysates.^{2,18,21,27} In cells fed with per-acetylated GalNAc analogues Ac₄GalNAzMe **1**
192 and Ac₄GalNPrAz **2**, both sugar precursors led to a dose-dependent increase in
193 fluorescence signal in cells expressing AGX1^{F383A} and NahK (Fig. 3A). The minimal
194 concentration required for visible signal after Ac₄GalNAzMe **1** feeding was 25 μ M.
195 We observed substantial background fluorescence signal in cell lines fed with
196 Ac₄GalNAzMe **1**, particularly at concentrations above 50 μ M. We attributed this
197 signal to non-enzymatic S-glyco-modification as a side product seen with per-
198 acetylated bioorthogonal sugars described by Chen and colleagues.^{25,26} However,
199 glycosylation in cells expressing NahK/AGX1^{F383A} led to a clear increase of
200 fluorescence intensity that was specific to individual glycoprotein bands, for instance
201 those at approximately 100 kDa. We attributed this signal to the mucin-like
202 glycoprotein CD43 that is heavily expressed in K-562 cells and chemically tagged by
203 GalNAzMe.^{2,28} Cells expressing NahK and AGX1^{F383A} showed visible fluorescent
204 signal when fed more than 2.5 μ M Ac₄GalNPrAz **2**. In the absence of NahK, feeding
205 with Ac₄GalNPrAz **2** also led to a dose-dependent fluorescence signal above a
206 minimum concentration of 12.5 μ M Ac₄GalNPrAz **2**. Incorporation of GalNPrAz was
207 observed in a much larger range of glycoproteins than GalNAzMe, commensurate
208 with UDP-GalNPrAz being epimerized into UDP-GlcNPrAz that could be used by
209 GlcNAc transferases.² In experiments comparing the labelling intensity of optimal
210 Ac₄GalNAzMe **1**/Ac₄GalNPrAz **2** concentrations, we further found that
211 overexpression of WT-AGX1 alone or together with NahK does not lead to
212 discernible fluorescence signal (Fig. 3B). Ac₄GalNAzMe **1** feeding required both
213 NahK and AGX1^{F383A} for bioorthogonal tagging whereas Ac₄GalNPrAz **2** requires at
214 least AGX1^{F383A}. These data were corroborated in two other cell lines, the murine
215 green fluorescent protein (GFP)-expressing 4T1 murine cancer cell line (4T1-GFP)

216 and the murine MLg fibroblast cell line (Supporting Fig. 4). Both cell lines
217 incorporated GalNPrAz and GalNAzMe into their glycoproteomes when expressing
218 both NahK and AGX1^{F383A}, but not when left untransfected, further confirming that
219 both biosynthetic enzymes lead to reproducible bioorthogonal tagging of the
220 glycoproteome.

221 The nature of glycoproteins into which GalNPrAz and GalNAzMe had been
222 incorporated was subsequently investigated. Lysates of cells expressing both NahK
223 and AGX1^{F383A} fed with per-acetylated GalNAc analogues were incubated with a
224 panel of glycosidases and glycoproteases (Fig. 3C). The well-characterized,
225 promiscuous GalNAc analogue Ac₄GalNAz served as a control to compare labelling
226 band patterns by in-gel fluorescence.¹⁵ The mucinase SmE was recently
227 demonstrated to cleave the protein backbone of mucin-domain glycoproteins with
228 broad tolerance for dense glycosylation and high glycan complexity.²⁹ Using SmE,
229 the 100 kDa fluorescent glycoprotein band disappeared across samples fed either
230 Ac₄GalNAzMe **1**, Ac₄GalNPrAz **2** or Ac₄GalNAz. A new band appeared at
231 approximately 90 kDa which we attributed to be a digestion product of CD43. A
232 commercial endo- α -N-acetylgalactosaminidase was next used to remove short core
233 1 O-glycans in the presence of a neuraminidase.³⁰ This treatment also led to
234 disappearance of the 100 kDa band across samples fed with all sugars, with the
235 emergence of a new band at approx. 70 kDa that likely lacks untagged O-glycans.
236 PNGaseF removed N-linked glycans from glycoproteins. The band corresponding to
237 CD43 at approximately 100 kDa remained in all samples, though appeared to be
238 shifted to a slightly lower molecular weight (Ac₄GalNPrAz **2** treated) or slightly higher
239 molecular weight (Ac₄GalNAzMe **1** treated). CD43 is known to carry a single N-
240 glycan,²⁸ the removal of which may impact the charge state of CD43 and thus its
241 migration by electrophoresis. Bands observed at approx. 60, 160 and 260 kDa in
242 cells treated with either Ac₄GalNPrAz **2** or Ac₄GalNAz disappeared upon PNGase F
243 treatment, suggesting cleavage of fluorescently labelled N-glycans. Taken together,
244 these results suggest GalNPrAz and GalNAzMe are indeed incorporated into mucin-
245 type O-glycans, and that Ac₄GalNPrAz **2** recapitulates the labelling of N- and O-
246 glycoproteins of Ac₄GalNAz.



247

248

249

250

251

252

253

254

255

Fig. 3: Cell surface incorporation and cell-specific bioorthogonal tagging of azidosugars. *A*, dose-dependent incorporation of GalNAzMe (left) and GalNPrAz (right) into the cell surface glycoproteome of stably transfected K562 cells as assessed by in-gel fluorescence. Cells were fed with the indicated concentrations of compounds **1** or **2**, subjected to cell-surface CuAAC with CF680-alkyne and glycosylation detected by fluorescence scanning. Data are one representative out of two independent replicates. *B*, comparison of stably transfected K562 cell lines for incorporation of GalNAzMe or GalNPrAz based on optimised feeding concentrations. Data are one representative out of two independent replicates. *C*, comparison of different glycoprotease or glycosidase digestions on lysates

256 of cells expressing both NahK and AGX1F383A fed with per-acetylated GalNAc analogues assessed
257 by in-gel fluorescence.

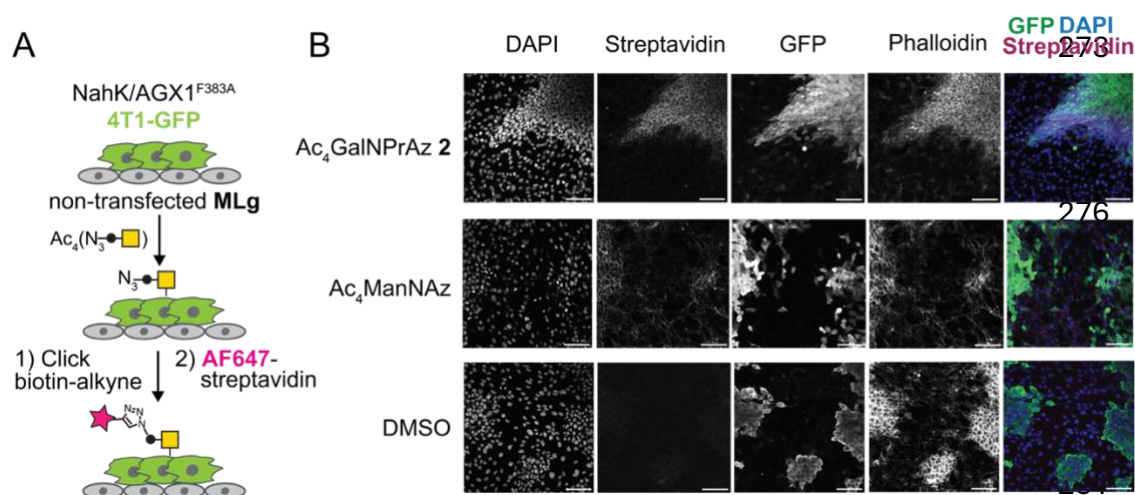
258

259 Expanding the monosaccharide repertoire for cell-specific bioorthogonal 260 tagging of glycoproteins

261

262 We next tested whether GalNPrAz and GalNAzMe are suitable substrates for
263 BOCTAG, employing a co-culture system between 4T1-GFP and MLg cells.¹⁷ 4T1-
264 GFP cells were transfected with NahK and AGX1^{F383A} or with an empty plasmid, and
265 grown in a co-culture system with non-transfected MLg cells. The co-culture was fed
266 with either Ac₄GalNAzMe **1**, Ac₄GalNPrAz **2**, or the more promiscuous reagent
267 Ac₄ManNAz that enters the pool of *N*-acetylneuraminic acid.³¹ Incorporation of a
268 clickable fluorophore allowed visualization of cell-surface glycosylation (Fig. 4A). We
269 found that only 4T1-GFP cells expressing the BOCTAG enzymes NahK/AGX1^{F383A}
270 efficiently incorporated GalNPrAz, leading to cell-specific bioorthogonal tagging of
271 glycoproteins (Fig. 4B).

272



282

283 **Fig. 4:** Cell-specific bioorthogonal tagging of glycoproteins with GalNPrAz. A, schematic describing
284 set-up of co-culture system between stably transfected 4T1-GFP cancer cells and MLg murine
285 fibroblasts. Cells were fed with compound **2** (62.5 μM), Ac₄ManNAz (10 μM) or an equivalent volume
286 of DMSO, subjected to on-cell CuAAC with biotin-alkyne, and imaged using fluorescently labelled
287 streptavidin. B, Microscopy data from one experiment. Scale bar set to 100 μm.

288

289 In contrast, Ac₄ManNAz feeding led to ubiquitous cell surface fluorescence on all cell
290 lines. In contrast, we observed no discernible cell-specific fluorescent labelling with

291 Ac₄GalNAzMe, indicating that labelling intensity was too weak for fluorescence
292 microscopy (Supporting Fig. 5). These data are consistent with our previous findings
293 suggesting that GalNAzMe requires further boosting of signal through engineered
294 glycosyltransferases.² We concluded that Ac₄GalNPrAz **2** allows for cell-specific
295 bioorthogonal tagging of glycoproteins in the presence of the BOCTAG enzymes
296 NahK/AGX1^{F383A}.

298 **Conclusions**

299 Bioorthogonal labelling techniques have rapidly evolved over the last decades,
300 fuelled by the need to probe the glycome. In recent years, the field has started to
301 map the metabolic fates of bioorthogonal monosaccharides, including their
302 compatibilities with biosynthetic enzymes as well as incorporation into different parts
303 of the glycome. Such metabolic precision is essential to allow the use of metabolic
304 tools in biomedical research. For instance, we have previously shown that
305 GalNAzMe allows investigation of the O-GalNAc glycoproteome in a genome-wide
306 genetic knockout screen.² In contrast, GalNPrAz is poised to enter O-GalNAc
307 glycans as well as other cellular glycans, presumably N-glycans. This finding renders
308 GalNPrAz a more promiscuous tool with higher incorporation efficiency, similar to the
309 alkynoate-containing sugar GalNAIk.²¹

310 Various strategies have been employed to allow for cell-specific chemical tagging of
311 proteins, including the use of biotin ligases and unnatural amino acids that directly
312 modify the peptide sequence.^{32–34} BOCTAG is complementary to these techniques,
313 targeting glycans as a ubiquitous PTM. Application of the BOCTAG tactic to
314 monosaccharides that enter different glycan subtypes further expands the toolbox for
315 cell-specific labelling of glycoproteins, employing accessible per-acetylated
316 monosaccharide precursors for convenient use in biomedical research.

318 **Acknowledgements**

319 This work was supported by the Francis Crick Institute which receives its core
320 funding from Cancer Research UK (CC2127), the UK Medical Research Council
321 (CC2127), and the Wellcome Trust (CC2127). This work was funded by the UK
322 Biotechnology and Biological Sciences Research Council (BB/V008439/1 and
323 BB/V014862/1 to B.S.) and Cancer Research UK (DRCMDP-Nov22/100011 to B.
324 S.). A. Z. is supported by a PhD studentship funded by the EPSRC Centre for

325 Doctoral Training in Chemical Biology - Innovation for the Life Sciences
326 EP/S023518/1 and Vertex Pharmaceuticals. S. A. M. is supported by the Yale
327 Science Development Fund. V. C. is supported by an NSF GRFP.

328

329 **Competing Interests**

330 S.A.M. is a consultant for InterVenn Biosciences and Arkuda Therapeutics, and a
331 coinventor on a Stanford nonprovisional utility patent application that has been filed
332 and is pending in the US (number US20220003777) related to the use of mucinases
333 for mass spectrometry analysis of mucin-domain glycoproteins.

334

335 **References**

336

- 337 1 N. J. Agard, J. A. Prescher and C. R. Bertozzi, *J. Am. Chem. Soc.*, 2004, **126**, 15046–
338 15047.
- 339 2 M. F. Debets, O. Y. Tastan, S. P. Wisnovsky, S. A. Malaker, N. Angelis, L. K. R. Moeckl, J.
340 Choi, H. Flynn, L. J. S. Wagner, G. Bineva-Todd, A. Antonopoulos, A. Cioce, W. M.
341 Browne, Z. Li, D. C. Briggs, H. L. Douglas, G. T. Hess, A. J. Agbay, C. Roustan, S. Kjaer,
342 S. M. Haslam, A. P. Snijders, M. C. Bassik, W. E. Moerner, V. S. W. Li, C. R. Bertozzi and
343 B. Schumann, *Proc. Natl. Acad. Sci. U.S.A.*, 2020, **117**, 25293–25301.
- 344 3 M. Kufleitner, L. M. Haiber and V. Wittmann, *Chem. Soc. Rev.*, 2023, **52**, 510–535.
- 345 4 C. G. Parker and M. R. Pratt, *Cell*, 2020, **180**, 605–632.
- 346 5 J. Hassenrück and V. Wittmann, *Beilstein J. Org. Chem.*, 2019, **15**, 584–601
- 347 6 L. M. Haiber, M. Kufleitner and V. Wittmann, *Front. Chem.*, 2021, **9**, DOI:
348 10.3389/fchem.2021.654932.
- 349 7 J. E. G. A. Dold, J. Pfozter, A. K. Späte and V. Wittmann, *ChemBioChem*, 2017, **18**, 1242–
350 1250.
- 351 8 A. K. Späte, H. Bußkamp, A. Niederwieser, V. F. Schart, A. Marx and V. Wittmann,
352 *Bioconjug. Chem.*, 2014, **25**, 147–154.
- 353 9 L. A. Bateman, B. W. Zaro, K. N. Chuh and M. R. Pratt, *Chem. Commun.*, 2013, **49**, 4328–
354 4330.
- 355 10 K. N. Chuh, B. W. Zaro, F. Piller, V. Piller and M. R. Pratt, *J. Am. Chem. Soc.*, 2014, **136**,
356 12283–12295.
- 357 11 J. Yang, J. Šečkute, C. M. Cole and N. K. Devaraj, *Angew. Chem., Int. Ed.*, 2012, **51**,
358 7476–7479.
- 359 12 D. M. Patterson, L. A. Nazarova, B. Xie, D. N. Kamber and J. A. Prescher, *J. Am. Chem.*
360 *Soc.*, 2012, **134**, 18638–18643.
- 361 13 P. V. Chang, X. Chen, C. Smyrniotis, A. Xenakis, T. Hu, C. R. Bertozzi and P. Wu, *Angew.*
362 *Chem., Int. Ed.*, 2009, **48**, 4030–4033.
- 363 14 D. J. Voadlo, H. C. Hang, E. J. Kim, J. A. Hanover and C. R. Bertozzi, *Proc. Natl. Acad.*
364 *Sci. U.S.A.*, 2003, **100**, 9116–9121.
- 365 15 H. C. Hang, C. Yu, D. L. Kato and C. R. Bertozzi, *Proc. Natl. Acad. Sci. U.S.A.*, 2003, **100**,
366 14846–14851.
- 367 16 M. Boyce, I. S. Carrico, A. S. Ganguli, S. H. Yu, M. J. Hangauer, S. C. Hubbard, J. J.
368 Kohler and C. R. Bertozzi, *Proc. Natl. Acad. Sci. U.S.A.*, 2011, **108**, 3141–3146.
- 369 17 A. Cioce, B. Calle, T. Rizou, S. C. Lowery, V. L. Bridgeman, K. E. Mahoney, A. Marchesi,
370 G. Bineva-Todd, H. Flynn, Z. Li, O. Y. Tastan, C. Roustan, P. Soro-Barrio, M. R. Rafiee, A.
371 Garza-Garcia, A. Antonopoulos, T. M. Wood, T. Keenan, P. Both, K. Huang, F.
372 Parmeggian, A. P. Snijders, M. Skehel, S. Kjær, M. A. Fascione, C. R. Bertozzi, S. M.

373 Haslam, S. L. Flitsch, S. A. Malaker, I. Malanchi and B. Schumann, *Nat. Commun.*, 2022,
374 **13**, 1–18.

375 18 B. Schumann, S. A. Malaker, S. P. Wisnovsky, M. F. Debets, A. J. Agbay, D. Fernandez, L.
376 J. S. Wagner, L. Lin, Z. Li, J. Choi, D. M. Fox, J. Peh, M. A. Gray, K. Pedram, J. J. Kohler,
377 M. Mrksich and C. R. Bertozzi, *Mol. Cell*, 2020, **78**, 824-834.

378 19 A. R. Batt, B. W. Zaro, M. X. Navarro and M. R. Pratt, *ChemBioChem*, 2017, **18**, 1177–
379 1182.

380 20 X. Fan, Q. Song, D. en Sun, Y. Hao, J. Wang, C. Wang and X. Chen, *Nat. Chem. Biol.*,
381 2022, **18**, 625–633.

382 21 A. Cioce, G. Bineva-Todd, A. J. Agbay, J. Choi, T. M. Wood, M. F. Debets, W. M. Browne,
383 H. L. Douglas, C. Roustan, O. Y. Tastan, S. Kjaer, J. T. Bush, C. R. Bertozzi and B.
384 Schumann, *ACS Chem. Biol.*, 2021, **16**, 1961–1967.

385 22 T. Keenan, F. Parmeggiani, J. Malassis, C. Q. Fontenelle, J. B. Vendeville, W. Offen, P.
386 Both, K. Huang, A. Marchesi, A. Heyam, C. Young, S. J. Charnock, G. J. Davies, B.
387 Linclau, S. L. Flitsch and M. A. Fascione, *Cell Chem. Biol.*, 2020, **27**, 1199-1206.

388 23 S. H. Yu, M. Boyce, A. M. Wands, M. R. Bond, C. R. Bertozzi and J. J. Kohler, *Proc. Natl.*
389 *Acad. Sci. U.S.A.*, 2012, **109**, 4834–4839.

390 24 F. V. De León González, M. E. Boddington, J. M. Kofsky, M. I. Prindl and C. J. Capicciotti,
391 *ACS Chem. Biol.*, 2024, **19**, 629–640.

392 25 K. Qin, H. Zhang, Z. Zhao and X. Chen, *J Am Chem Soc*, 2020, **142**, 9382–9388.

393 26 W. Qin, K. Qin, X. Fan, L. Peng, W. Hong, Y. Zhu, P. Lv, Y. Du, R. Huang, M. Han, B.
394 Cheng, Y. Liu, W. Zhou, C. Wang and X. Chen, *Angew. Chem., Int. Ed.*, 2018, **57**, 1817–
395 1820.

396 27 Z. Li, L. Di Vagno, A. N. Cheallaigh, D. Sammon, D. C. Briggs, N. Chung, V. Chang, K. E.
397 Mahoney, A. Cioce, L. D. Murphy, Y.-H. Chen, Y. Narimatsu, R. L. Miller, L. I. Willems, S.
398 A. Malaker, G. J. Miller, E. Hohenester and B. Schumann, *bioRxiv*, 2023, DOI:
399 10.1101/2023.12.20.572522.

400 28 S. R. Carlsson and M. Fukuda, *J. Biol. Chem.*, 1986, **261**, 12779–12786.

401 29 J. Chongsaritsinsuk, A. D. Steigmeyer, K. E. Mahoney, M. A. Rosenfeld, T. M. Lucas, C.
402 M. Smith, A. Li, D. Ince, F. L. Kearns, A. S. Battison, M. A. Hollenhorst, D. Judy Shon, K.
403 H. Tiemeyer, V. Attah, C. Kwon, C. R. Bertozzi, M. J. Ferracane, M. A. Lemmon, R. E.
404 Amaro and S. A. Malaker, *Nat. Commun.*, 2023, **14**, 1–18.

405 30 I. Bagdonaite, S. A. Malaker, D. A. Polasky, N. M. Riley, K. Schjoldager, S. Y. Vakhrushev,
406 A. Halim, K. F. Aoki-Kinoshita, A. I. Nesvizhskii, C. R. Bertozzi, H. H. Wandall, B. L.
407 Parker, M. Thaysen-Andersen and N. E. Scott, *Nat. Rev. Methods Primers*, 2022, **2**, 48.

408 31 J. A. Prescher, D. H. Dube and C. R. Bertozzi, *Nature*, 2004, **430**, 873–877.

409 32 W. Wei, N. M. Riley, A. C. Yang, J. T. Kim, S. M. Terrell, V. L. Li, M. Garcia-Contreras, C.
410 R. Bertozzi and J. Z. Long, *Nat. Chem. Biol.*, 2021, **17**, 326–334.

411 33 B. Alvarez-Castelao, C. T. Schanzenbacher, C. Hanus, C. Glock, S. tom Dieck, A. R.
412 Dörrbaum, I. Bartnik, B. Nassim-Assir, E. Ciirdaeva, A. Mueller, D. C. Dieterich, D. A.
413 Tirrell, J. D. Langer and E. M. Schuman, *Nat. Biotechnol.*, 2017, **35**, 1196–1201.

414 34 S. Kehroesser, O. Cast, T. S. Elliott, R. J. Ernst, A. C. Machel, J. X. Chen, J. W. Chin and
415 M. L. Miller, *PNAS Nexus*, 2023, **2**, 1-12.

416